

Multiscale analysis of geomagnetic disturbances: case study

Margarete Oliveira Domingues, Odím Mendes,

LAC/CTE, DGE/CEA

Brazilian Institute for Space Research - INPE

12201-970, São José dos Campos, São Paulo, Brazil

E-mail: margarete@lac.inpe.br, odim@dge.inpe.br,

Abstract: *Geomagnetic storms are recognized as a worldwide decrease of the horizontal component of the Earth's magnetic field measured at middle and low latitude magnetometers. Those disturbances can be viewed in general as a result of a chain of electrodynamic processes from the Sun to the Earth. In this work the behavior of raw magnetometer data recorded at Kakioka magnetic station, with one minute time resolution, related to periods of magnetic storms were analyzed. The methodology applied consists in the use of the orthogonal discrete wavelet transform applied to magnetometer data in order to identify the storm period using a multi-scale hard and soft threshold set of the wavelet coefficients. The wavelet coefficients amplitudes of the first three orthogonal wavelet decomposition levels using a proper threshold allow to characterize the period of the main phase of geomagnetic storms, taking into account the amount of energy of the transients during this period. The purpose is to identify the main phase according the temporal regularity of H-component of magnetic field, because in that moment the transient features are specially related to the energetic transfer process from solar plasma to the magnetosphere. An example of this kind of result is showed here.*

keywords: *Earth's magnetosphere Sun–Earth coupling geomagnetic storm Dst index wavelet analysis*

1 Introduction

The geomagnetic disturbances are consequence of the electro-dynamical interaction between solar wind and the magnetosphere. The principal property of geomagnetic storms — which are recognized as a worldwide decrease of the horizontal component of the Earth's magnetic field measured at middle and low latitude magnetometers — is related to the enhancement of an electric current flowing toroidally around the Earth, centered at the equatorial plane and at altitudes of 2 to 7 Earth's radii (ER). Such ring current is formed by ions, mostly protons and oxygen ions from the ionosphere, and electrons in the 10 – 300 keV energy range, which are trapped by the Earth's geomagnetic field. The ring current concentrates in the equatorial region of the Earth's magnetosphere and produces a magnetic field disturbance opposite to the Earth dipole field direction. The primary causes of geomagnetic storms at the Earth's surface are the strong dawn-to-dusk electric fields associated with the presence of a southward directed Interplanetary Magnetic Field (IMF) in the vicinities of the Earth. Geomagnetic storms and sub-storms are closely related, in the sense that both can be developed when the interplanetary magnetic field has a strong southward component [4, 5].

Looking the Dst hourly index dataset, presented in [6], in these wavelet point of view, one can observe that this index is highly influenced by Kakioka more than the others three stations

that are used to create the index. Dst is an index calculated from the magnetic records from selected stations and represents a general behavior of a depression in the magnetic fields measured close to the middle-to-low latitudes. More complete details on this index is presented in [7]. In [6] several magnetic stations are studied in the wavelet analysis on a moderate storm. In this work we extended that analysis using much more storms, with different intensity, however for just Kakioka geomagnetic station (known shortly as KAK). In this study we use the first three wavelet decomposition levels of the horizontal component of the Earth magnetic field, defined as H-component, to help in the automatic identification of the main phase of geomagnetic storms, which is the moment between the beginning and the minimum of the geomagnetic depression. This kind of identification could have a practical importance in the Space weather monitoring system or as a tool to automatically find the energetic injection period of these events in a long term data base.

This paper is organized as follows. In the next section, the dataset is presented briefly. After, the methodology is discussed. In Section 3, the results are discussed, followed by a last section with the final remarks.

2 Dataset & Methodology

2.1 Dataset

From 1997 to 2004, we study 52 magnetic storms (25 moderate ($-100 < \text{Dst} \leq -50$) and 14 intense ($-250 < \text{Dst} \leq -100$) and 14 super-intense), and in 1989 a super-storm ($\text{Dst} < -300$ nT). These time series are minutely dataset with 12 hours before the magnetic storm onset to the complete recovery of the signal. The selected periods varied from 3 to 7 days, depending on the characteristics and intensity of the magnetic storm. The storms studied are presented in the Table 1 in Section 3 with their respectively time of occurrence and Dst minimum value, the last given as amplitude. It identifies in a concise manner all those storms and characterizes the results of wavelet treatment. Each value n_j is the number of wavelet coefficients in each level j above the threshold, for the first three levels. \tilde{d}_j is the sum of the wavelet coefficients of level j squared, in which the level is for values above the threshold. It means how intense the magnetic records on surface are affected by the impulsive energy transfer. These first levels seem enough to guarantee the identification of the period of injection of energy, and consequently the main phase. A future work just in development will analyze the use of those features for now-casting purposes.

2.2 Discrete wavelet transforms

The discrete orthogonal wavelet transforms and their inverse are defined in details for instance in [1, 2]. This transform has the property of double localization: the wavelet coefficients d_k^j are a measure of the frequency information in the support of the wavelet function, where j indicates the scale and k the position. Consequently, the wavelet transform is a time-frequency transform with temporal resolution inversely proportional of the frequency. One can prove that the amplitude of the wavelet coefficient can be use to study local regularities of functions [1]. These are the main properties that we use in this work. In Figure 1 there is an example of a function and its scale-position plane ($j \times x$ plane) showing the position of the wavelet coefficients greater than 10^{-5} . One can observe that in this kind of visualization is possible to identify the local discontinuities in the function.

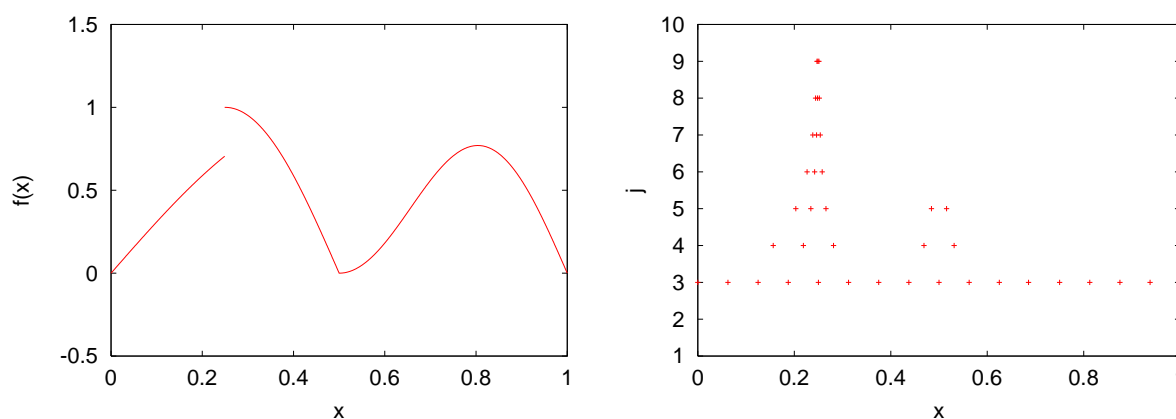


Figure 1: Example of a function $f(x)$ and its $j \times x$ plane after a certain thresholding. In this function there is a discontinuity and a discontinuity on the first derivative. In that regions, one can observe that the larger magnitude of the wavelet coefficients reaches larger scales j than in the others regions, *i.e.* these coefficients can be used as an index of the regularity of an analyzing function.

2.3 Orthogonal Properties & Energy Conservation

On the discrete orthogonal wavelet transform theory, there is a Energy Conservation Theorem, a generalization of Parseval Theorem from Fourier Analysis, *i.e.*, the sum of squared of the dataset must be the same of the sum of scale and wavelet coefficients. We use this property to choose the cut-off limits of the squared wavelet coefficients and to measure the total "energy" remained in the three first levels of the decompositions.

Choice of the wavelet

In the applications of this paper we use a wavelet function that represent locally linear approximation, which means that we are interested in a "shock" like perturbation in the geomagnetic field, namely Daubechies order 2 (*i.e.*, using 4 coefficients for the low-pass filter). A more detailed discussion about the choice of the proper wavelet to be used can be found in [3].

Thresholding as an indicator index

Here we consider the squared amplitude of the wavelet coefficients d^j . It is given in arbitrary units which are the same for the three decomposition levels. Proper details in a non short presentation can be found in [6]. These three levels ($j = 1, 2, 3$) are associated to some pulsation frequencies well known in space geophysics, identifying the main phase period because they are related to the energy transfer process. We applied a three level decomposition of an orthogonal wavelet transform to Kakioka magnetometers (1 D time series). After we identify the time where the wavelet coefficients are larger than a global base line and apply a hard thresholding process. More precisely, the threshold set 1, 2, 4 are the lowest values that still allow unambiguously the identification of the magnetic storm. Any threshold set above the limit that can distinguish the background from the magnetic field signal, could, in principle, be used since it does not overtake the ability of the tool to point out the magnetic disturbance associated with the storm period. It is worth to notice that the observed thresholds are specific to Kakioka at Japan (KAK) station. The threshold sets may vary from station to station [6].

2.4 Identification of the main phase of storms

Those time intervals with the wavelet coefficient exceeding the threshold are the candidate regions to identify the main phase of storms, because they identify the period of transients in the magnetic records on Earth's surface. Indeed, there are many other possibilities to define the most proper thresholds and research in this subject are still required. In general, the first step is to perform the wavelet transform, then someone choose a threshold, and reconstruct the data series with the wavelet coefficient bigger than the defined threshold.

2.5 Summary

The methodology applied can be briefly summarized as follow. Starting from records of a magnetometer (for instance, from Kak station in this work), the wavelet signatures were obtained for each event. A hard thresholding process was applied to the first three decomposition levels and the wavelet coefficients above the threshold were counted. The energy accumulated in these peaks was then integrated and a well established positive correlation between Dst and the number of peaks and accumulated energy allowed a straightforward identification of the storm intensity, which is related to the main phase of the storm.

3 Results and Discussion

In this analysis it was found empirically that 2^{j-1} could be used as a hard threshold for the squared wavelet coefficients set of values for the $j = 1, 2, 3$ decomposition levels to identify the main phase period of the geomagnetic storm. We also study quiet periods around these storms studied here and we verify that their wavelet coefficients have much less amplitude than the ones in the main phase the storms or during new entrance of energy. From the overall observed events we notice that the shocks (transients) are detected simultaneously in all the decomposition levels, however the number of wavelet coefficients and their amplitudes can vary considerable from one level to the other. As an example, the integrate values of the squared wavelet coefficients \tilde{d}^j normalized by the number of squared wavelet coefficients n^j above the threshold is presented in the Table 1.

To illustrate this case studies, we presented in this work the graphics used in a practical visualization of these identifications for three different kinds of storms in Figure 2. It shows an example of the H component of the geomagnetic field measured at KAK station, and the significant wavelet coefficients of the first three decomposition levels for, respectively, the moderate, intense and super-intense geomagnetic storms. Here the squared wavelet coefficient is presented. From the overall observed events it is possible to notice that the shocks are detected simultaneously in all the decomposition levels. However the number of wavelet coefficients and their amplitudes can vary considerable from one level to the other. Note that the main phase of a storm period is identified by the highest wavelet coefficients that occur ordinarily during the transient period. This behavior is observed in all the cases studied, and in quiet periods there are not significant wavelet coefficient. To illustrate this conclusion, for all storms studies, presented in Table 1, the wavelet coefficients energy above the threshold was compared to the main phase energy defined by Dst index. One can observed that there is an agreement between them.

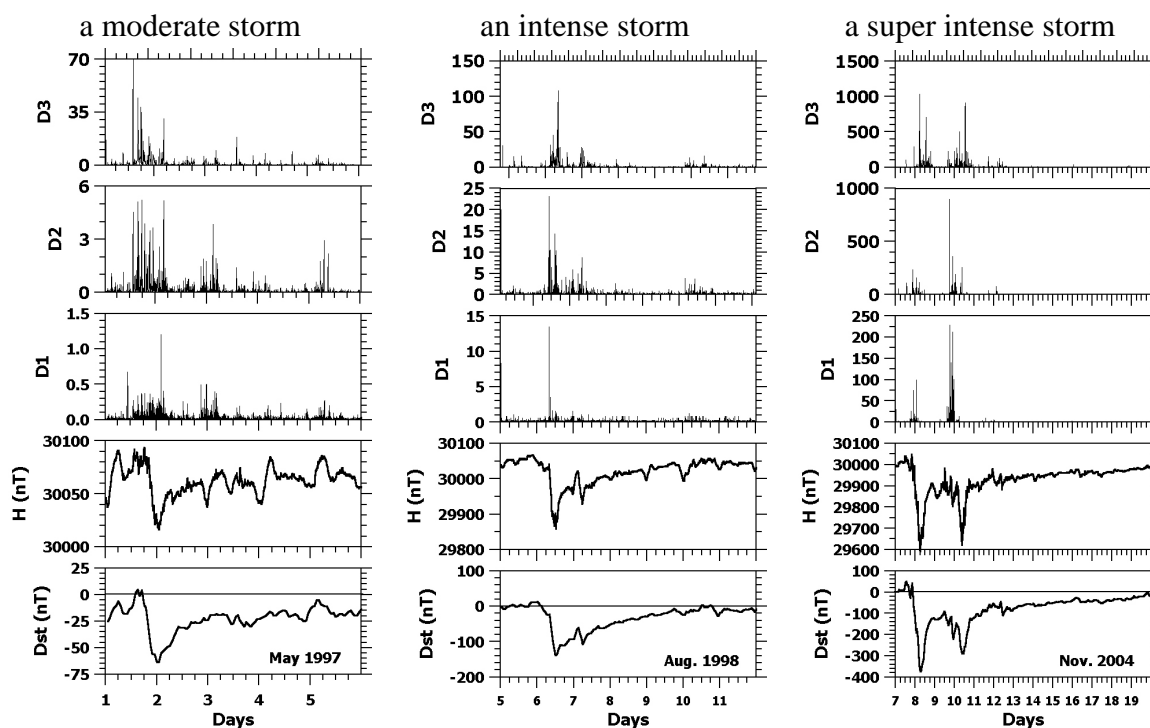


Figure 2: Illustration of the typical wavelet detection for (a) a moderate storm, this case represents the storm of May 2, 1997 ($Dst = -64nT$). (b) an intense storm, this case represents the storm of Aug. 6, 1998 ($Dst = -138nT$), and (c) a super intense storm, this case represents the storm of Nov. 8, 2004 ($Dst = -373nT$).

4 Final Remarks

With this study we verified that using the wavelet coefficients calculated from magnetic records (for instance here from the magnetometer at Kakioka magnetic station) was possible to identify the main phase of a geomagnetic storm in a similar manner of using the post-processed Dst index. Dealing with the raw data presenting all features of the original signal, as is in this wavelet applications, is better than to use a modified data in a post-processing treatment, as is in the Dst index.

An important result that came out from the overall this analysis was that there exist a wavelet signature that clearly identifies the main phase of a geomagnetic storm period, for moderate, intense and super intense magnetic storms. The fact that we are detecting a sequence of transient field variations, interpreted as ring current oscillations and disturbances in other magnetospheric electrical current systems, can be a very convenient indication for some kinds of energy transports, that occurs through this electro-dynamical coupling between solar plasma and the Earth's atmosphere, that contribute to the field variations measured on the ground. These chain of effects will be treated in further studies.

In all the cases studied, the shocks mostly found in the main phase, were related potentially to an enhancement in the population of the ring current, confirming the results obtained for moderate storms. The signatures are characterized by the amplitude and the amount of the wavelet coefficients above the thresholds determined empirically. It was also noticed that some storms classified as moderate storms presented unexpected high amplitude coefficients, while some intense storms presented lower amplitude coefficients. An study of this behavior could be done in order to verify the complexity processes involved in these storms that may be the

usual classification using exclusively Dst index, which is not able to detect those features. For dealing directly with row data and by identifying complex features, the authors believe that the methodology developed here, even seen as a tool, could be of a great help in a comprehensive characterization of the intrinsic processes that characterize the geomagnetic storms, adding to the use of the Dst index. Mainly because of the recent space weather challenges the determination of general trends and characteristics of the magnetosphere activities generated by different solar wind drivers can be seen as a step forward in understanding the complex issue of the Earth's magnetosphere electrodynamics.

References

- [1] I. Daubechies. *Ten lectures on wavelets*, volume 61 of *Series in Applied Mathematics*. (SIAM), Philadelphia, PA, 1992.
- [2] M. O. Domingues. *Análise Wavelet na Simulação Numérica de Equações Diferenciais Parciais com Adaptabilidade Espacial*. PhD thesis, Universidade Estadual de Campinas, UNICAMP, Brasil., 2001.
- [3] M. O. Domingues, O. Jr. Mendes, and A. Mendes da Costa. On wavelet techniques in Atmospheric Sciences. *Advances in Space Research*, 35(5):812–819, May 2005.
- [4] W. D. Gonzalez, J. A. Joselyn, Kamide Y., H. W. Kroehl, G. Rostoker, B. T. Tsurutani, and V. M. Vasyliunas. What is a geomagnetic storm? *Journal of Geophysical Research*, 99(A4):5771–5792, APR 1994.
- [5] O. Mendes. *A origem interplanetária e o desenvolvimento da fase principal das tempestades geomagnéticas moderadas (1978-1979)*. PhD thesis, INPE, São José dos Campos, 1992.
- [6] O. Mendes, M. O. Domingues, A. Mendes da Costa, and A. L. Clúa de Gonzalez. Wavelet analysis applied to magnetograms: Singularity detections related to geomagnetic storms. *Journal of Atmospheric and Terrestrial Physics*, 67:1827–1836, Dec 2005. [SPECIAL ISSUE].
- [7] O. Mendes, A. Mendes da Costa, and F.C.P. Bertoni. Effects of the number of stations and time resolution on dst derivation. *Journal of Atmospheric and Solar-Terrestrial Physics*, 68(18):2127–2137, 2006.

5 Acknowledgments

This work was supported by CNPq (process number 309017/2007-6, 486165/2006-0 and 308680/2007-3, 478707/2003, 477819/2003-6, 382465/01-6), FAPESP (process number 2007/07723-7) and CAPES (process number 86/2010-29). The authors wish to thank SPIDR-Boulder and WDC-Kyoto for the datasets used in this work. We are grateful to Varlei E. Menconi for their helpful computational assistance.

Table 1: Study magnetic storms with their Dst index and integrate wavelet coefficients

year	month	day	Dst	d^1/n^1	d^2/n^2	d^3/n^3	n^1	n^2	n^3
89	03	13	589	25	58	160	557	431	331
97	01	10	78	34	46	89	1	23	38
97	02	17	54	24	43	48	1	1	1
97	03	28	63	5	34	35	1	3	8
97	04	11	82	4	15	43	7	43	46
97	04	16	77	49	21	28	1	6	23
97	05	02	64	20	12	28	1	4	16
97	05	27	73	13	15	21	1	2	15
97	10	24	60	50	90	27	1	14	41
98	02	18	100	42	23	46	1	5	14
98	10	19	112	10	15	48	9	25	49
98	12	25	57	24	28	20	1	1	4
98	12	11	69	18	17	24	1	3	13
98	08	06	138	10	12	27	4	15	39
98	09	25	207	18	32	69	34	54	70
99	11	07	73	73	80	65	4	7	17
99	01	13	52	27	15	44	1	9	13
99	02	28	94	219	177	77	2	5	31
99	03	07	57	5	15	28	1	11	30
99	03	29	50	40	15	24	5	12	20
99	04	17	91	70	14	60	9	31	46
99	07	31	53	80	23	53	70	66	72
99	08	20	56	93	52	54	2	10	33
99	09	13	74	11	12	23	5	24	35
99	12	13	85	11	11	34	2	7	20
99	09	22	173	13	38	95	37	42	38
00	07	16	301	30	89	221	294	273	196
00	05	24	147	14	52	98	114	122	124
01	10	28	157	46	43	67	4	14	38
01	08	17	105	16	32	57	31	49	75
01	02	09	127	14	21	58	9	15	34
01	10	21	187	14	29	74	89	97	99
00	08	12	235	16	35	87	104	137	125
01	04	11	271	18	27	90	171	187	170
01	03	31	387	19	44	127	416	449	411
01	02	13	50	61	117	75	2	2	8
01	04	04	50	18	33	82	8	17	31
01	06	18	61	90	18	38	6	15	41
01	12	22	59	22	31	47	5	8	11
02	03	23	100	4	15	1.7	2	20	34
02	04	17	149	10	30	6.4	61	93	134
02	05	11	110	10	30	6.4	17	37	47
02	05	23	109	21	72	1.9	51	54	52
02	08	01	102	5	14	3.3	13	46	79
02	08	18	105	6	20	2.6	9	23	57
02	09	04	181	14	36	5.4	158	134	183
02	10	01	160	98	69	5.7	8	24	77
02	10	14	100	50	15	2.4	1	10	23
03	05	30	131	14	37	114	220	214	166
03	06	16	145	10	15	44	24	8	91
03	08	17	168	12	22	39	39	81	141
04	07	27	197	14	28	109	160	239	267
04	11	08	383	18	34	66	263	247	278